Improved hole mobility and suppressed trap density in polymer-polymer dual donor based highly efficient organic solar cells

Vishal Bharti, Abhishek Sharma, Vinay Gupta, Gauri D. Sharma, and Suresh Chand

Citation: Applied Physics Letters **108**, 073505 (2016); doi: 10.1063/1.4942394
View online: http://dx.doi.org/10.1063/1.4942394
View Table of Contents: http://scitation.aip.org/content/aip/journal/apl/108/7?ver=pdfcov
Published by the AIP Publishing

Improved hole mobility and suppressed trap density in polymer-polymer dual donor based highly efficient organic solar cells

Vishal Bharti,[1,2] Abhishek Sharma,[1,2] Vinay Gupta,[1] Gauri D. Sharma,[1] and Suresh Chand[1,a)]

[1]*CSIR-Network of Institutes for Solar Energy, Organic and Hybrid Solar Cell Group, Physics of Energy Harvesting Division, CSIR-National Physical Laboratory, Dr. K. S. Krishnan Marg, New Delhi 110012, India*
[2]*Academy of Scientific and Innovative Research (AcSIR), CSIR-National Physical Laboratory, Dr. K. S. Krishnan Marg, New Delhi 110012, India*

(Received 3 November 2015; accepted 7 February 2016; published online 19 February 2016)

Here we report, the charge transport properties of polymer-polymer dual donor blended film, viz., polythieno[3,4-b]-thiophene-co-benzodithiophene (PTB7) and poly [N-9″-hepta-decanyl-2,7-carbazole-alt-5,5-(4′,7′-di-2-thienyl-2′,1′,3′benzothiadiazole) (PCDTBT) in the optimized concentration. Trap density and hole mobility in polymer-polymer (PTB7-PCDTBT) dual donor system have been studied by means of current density–voltage *(J-V)* characteristics at various temperatures, i.e., 280 K–120 K in hole only device configuration, i.e., indium tin oxide/poly(3,4-ethylenedioxythiophene):poly(styrenesulphonate) (PEDOT:PSS)/Polymer film/gold (Au). The *J-V* curves exhibit the space charge limited conduction behavior. The corresponding hole mobility for PTB7 and PCDTBT are $3.9 \times 10^{-4}\,cm^2\,V^{-1}\,s^{-1}$ and $2.1 \times 10^{-4}\,cm^2\,V^{-1}\,s^{-1}$, respectively, whereas it is $9.1 \times 10^{-4}\,cm^2\,V^{-1}\,s^{-1}$ in the polymer-polymer blend of PTB7:PCDTBT (0.7:0.3). This enhancement in mobility can be attributed to the suppressed trap density in PTB7:PCDTBT (0.7:0.3) of $7.4 \times 10^{16}\,cm^{-3}$, as compared to the trap density of $1.1 \times 10^{17}\,cm^{-3}$ for PTB7 and $1.6 \times 10^{17}\,cm^{-3}$ for PCDTBT. Atomic force microscopy shows an improvement in the morphology of the blend. The *J–V* characteristic at various light intensities in the bulk heterojunction (BHJ) solar cell reveals that the blending of PCDTBT in PTB7 suppressed the trap-assisted recombination. The corresponding power conversion efficiencies for PTB7:$PC_{71}BM$, PCDTBT:$PC_{71}BM$ and PTB7:PCDTBT:$PC_{71}BM$ BHJ solar cells are 6.9%, 6.1% and 9.0%, respectively. This work unravels that the enhanced mobility and suppressed trap density play a significant role in the improvement of efficiency in dual donor based organic solar cells. © *2016 AIP Publishing LLC*. [http://dx.doi.org/10.1063/1.4942394]

Significant developments have been made in Bulk heterojunction (BHJ) polymer solar cells (PSCs), especially on low bandgap copolymers and power conversion efficiencies (PCEs) of over 10% achieved in single junction organic solar cells recently.[1,2] However, PCE is still limited by narrow light absorption range and low charge carrier mobilities of the polymers, which limits the short circuit current (J_{sc}) in the BHJ solar cells. To overcome this problem, ternary PSCs[3,4] have been developed to enhance the absorption range, increase the short circuit current (J_{sc}) and modulate the open circuit voltage (V_{oc}). Ternary PSCs consist of either two donor materials with one fullerene acceptor (D1:D2:A)[5–7] or one donor material with two fullerene acceptors (D:A1:A2).[8,9] These ternary blends exhibit charge transfer[5] or energy transfer.[6,10,11] It has been shown that the Förster Resonance Energy Transfer (FRET) effect on polymer-polymer poly[4,8-bis[(2-ethylhexyl) oxy]benzo[1,2-b:4,5-b′]dithiophene-2,6-diyl][3-fluoro-2-[(2-ethylhexyl) carbonyl] thieno[3,4-b]thiophenediyl] (PTB7); poly[9-(1-octylnonyl)-9H-carbazole-2,7-diyl]-2,5-thiophenediyl-2,1,3-benzothiadiazole-4,7-diyl-2,5-thiophenediyl] (PCDTBT) and [6,6]-phenyl C_{71} butyric acid methyl ester ($PC_{71}BM$) ternary blend system boosts the efficiency of conventional BHJ-PSCs.[6] Further, dual donor and multidonor systems show improved PCE in excess of 9% due to energy transfer and efficient charge transport.[7,12] However, the role of mobility and trap density in the improvement of charge transport has not been explored yet. Therefore, the aim of this work is to understand the role of charge transport, i.e., hole mobility (μ), trap density (N_t) and critical voltage (V_c) for improvement in the PCE of dual donor (PTB7-PCDTBT) based ternary solar cells.

The PTB7, PCDTBT and $PC_{71}BM$ were procured from 1-materials, Canada. For device fabrication, the indium tin oxide (ITO) glass substrates (sheet resistance = 15 Ω/□) were sonicated in soap solution, acetone and isopropanol. Cleaned ITO glasses were then exposed to ultraviolet-ozone irradiation for 15 min. A thin layer of PEDOT:PSS (Clevios PH) was spincoated at 4000 rpm for 40 s over ITO glass and dried at 150 °C in air for 30 min. Active layers were spin-coated using the solutions (chlorobenzene solvent with 25 mg/ml) at 1000–1500 rpm in a glove box. Finally, either aluminium (Al) electrode (∼100 nm) for BHJ devices or gold (Au) electrode (∼200 nm) for hole only devices was thermally deposited in high vacuum ($\sim 8 \times 10^{-7}$ mbar), over the active layer through shadow mask. The active area of the devices was ∼8 mm^2 in all the cases. The current density-voltage *(J-V)* characteristics of these devices were measured at different temperature with a Keithley 2420 Source Meter unit interfaced with a computer and liquid nitrogen based cryostat system.

a)Author to whom correspondence should be addressed. Electronic mail: schand@mail.nplindia.org

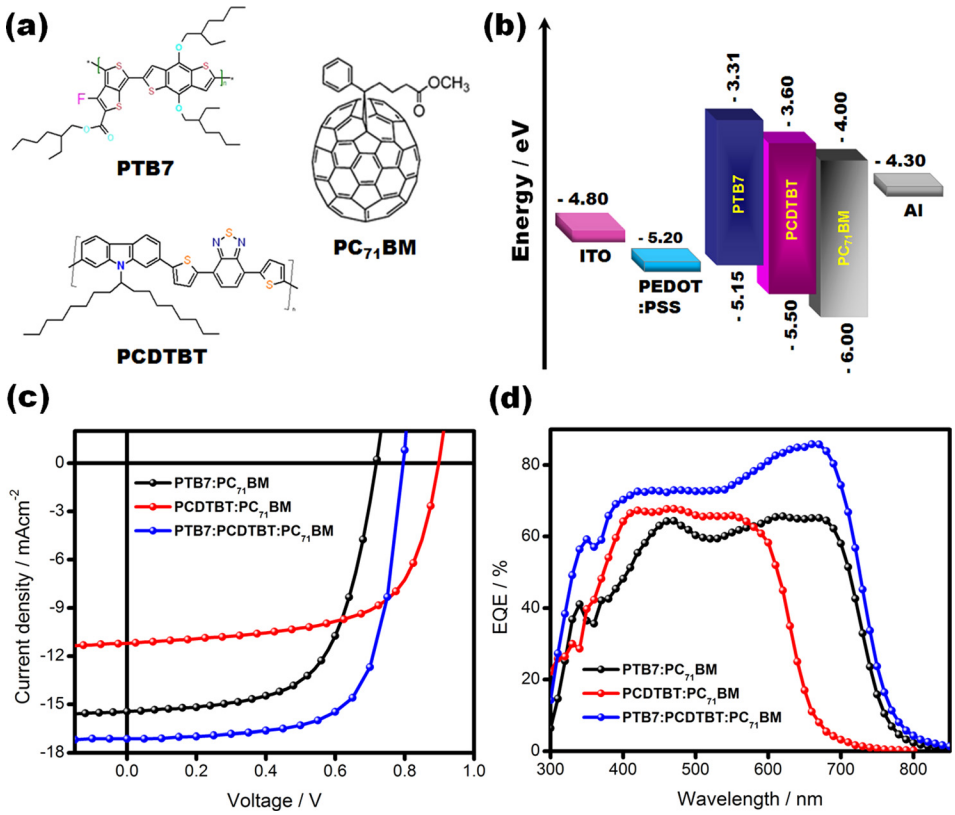

FIG. 1. (a) Molecular structures of PTB7, PCDTBT and $PC_{71}BM$. (b) Energy levels of materials used in the solar cell device. (c) and (d) Photovoltaic *J-V* characteristics and EQE measurement of the PTB7:$PC_{71}BM$, PCDTBT:$PC_{71}BM$ and PTB7:PCDTBT:$PC_{71}BM$ devices.

The photovoltaic performance of the binary blends PTB7:$PC_{71}BM$ (1:1.5), PCDTBT:$PC_{71}BM$ (1:4) and ternary blend PTB7:PCDTBT:$PC_{71}BM$ (0.7:0.3:2) BHJ solar cell devices was investigated by using conventional structure, i.e., ITO/poly(3,4-ethylenedioxythiophene):poly(styrenesulphonate) (PEDOT:PSS)/Active layer/Al. Figure 1(a) shows the chemical structure of PTB7, PCDTBT and $PC_{71}BM$ used in ternary structure, and Figure 1(b) shows the energy band diagram with the highest occupied molecular orbital (HOMO) and lowest unoccupied molecular orbital (LUMO) energy level of PTB7, PCDTBT, $PC_{71}BM$ and work functions of the various components of the solar cell. Figure 1(c) shows the photovoltaic *J-V* characteristics of the binary and optimized ternary BHJ solar cells under solar simulator AM 1.5 G with an intensity of 100 mW cm^{-2}. The solar cells with the binary blend of PTB7:$PC_{71}BM$ and PCDTBT:$PC_{71}BM$ show a PCE (η) of 6.9% and 6.1%, respectively, whereas the optimized ternary blend of PTB7:PCDTBT:$PC_{71}BM$ (0.7:0.3:2) shows a PCE of 9%. The photovoltaic performance parameters are shown in Table I. The corresponding external quantum efficiency (EQE) of the BHJ solar cells is shown in Figure 1(d). It is evident that the EQE of PTB7: PCDTBT:$PC_{71}BM$ (0.7:0.3:2) solar cell is increased to ~85% with respect to individual single donor PTB7:$PC_{71}BM$ (~70%) and PCDTBT:$PC_{71}BM$ (~60%) solar cells.

TABLE I. Photovoltaic performance parameters for the devices with different active layers.

Active layer	V_{OC} (V)	J_{SC} (mA cm^{-2})	*FF* (%)	PCE (%)	R_s Ω cm^2	R_{sh} kΩ cm^2
PTB7:$PC_{71}BM$	0.72	15.45	62.4	6.9	6.5	0.6
PCDTBT:$PC_{71}BM$	0.89	10.90	63.0	6.1	3.2	1.1
PTB7:PCDTBT:$PC_{71}BM$	0.80	17.25	65.5	9.0	1.5	1.7

To analyze the transport properties, i.e., μ, N_t, and V_c, we have measured the *J-V* characteristics of PTB7, PCDTBT and PTB7:PCDTBT (0.7:0.3) thin films in dark at various temperature range (280 K–120 K) in hole only device configuration, i.e., ITO/PEDOT:PSS/Polymer film/Au. The HOMO and LUMO energy levels of PTB7 and PCDTBT are −5.15, −5.5 eV, and −3.31, −3.6 eV, respectively. The work functions of Au ($\varphi \approx -5.1$ eV), ITO ($\varphi \approx -4.8$ eV) and PEDOT:PSS ($\varphi \approx -5.2$ eV) are closer to the HOMO and far below the LUMO energy level of PCDTBT and PTB7, thus the charge injection barrier is quite high towards LUMO, and the hole transport is dominated through the HOMO level only.

The *J-V* characteristics of the PTB7 and PCDTBT polymers and their blend were investigated using space charge limited conduction (SCLC) mechanism. It is well know that SCLC governs the charge transport in various ways, i.e., the trap model (drift of charge carriers under the influence of traps, exponential distribution of traps in energy space)[13–15] and the temperature/field dependent mobility models.[16,17] For hole only devices, the *J-V* curves of PTB7, PCDTBT and PTB7:PCDTBT (0.7:0.3) blends (Figures 2(a), 2(b), 2(c)) follow the trap model with exponential distribution of traps in energy space as discussed below.

At low applied bias, the *J-V* characteristics follow Ohm's law, because the injected hole density p is negligible compared to the density of thermally generated holes p_0 inside the specimen. This is exemplified by the following equation:[15]

$$J = qp_0\mu\frac{V}{d} > \frac{9}{8}\varepsilon\mu\frac{V^2}{d^3}, \quad (1)$$

where q is the electronic charge, μ is the carrier mobility, d is the thickness of the film and $\varepsilon = \varepsilon_0\varepsilon_r$ is the permittivity of

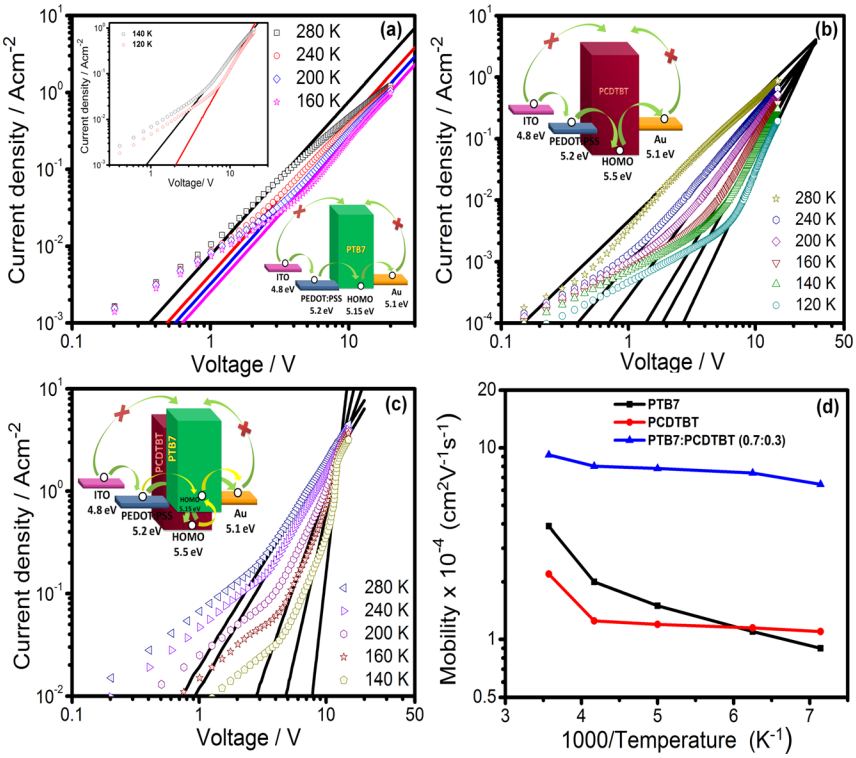

FIG. 2. Experimental (symbols) and calculated (solid lines) *J-V* characteristics of the hole only devices in the dark at different temperature range: (a) PTB7, (b) PCDTBT and (c) PTB7:PCDTBT (0.7:0.3). Top inset of (a) shows the *J-V* characteristics of the hole only devices at 140 K and 120 K. Insets (a)–(c) also show schematic energy level diagrams of devices. (d) Temperature dependence mobility of PTB7, PCDTBT and PTB7:PCDTBT (0.7:0.3) blend.

material. With the increase of applied voltage (field), the injected carrier density increases and at a point where it is equal to the thermally generated carrier density, the *J-V* characteristics follow the SCLC mechanism. The onset voltage (V_Ω) from ohm's law to SCLC is given by[15]

$$V_\Omega = \frac{8}{9}\frac{qp_0d^2}{\varepsilon}. \tag{2}$$

Pure SCLC with no traps is given by Mott's law[15]

$$J = \frac{9}{8}\varepsilon\mu\frac{V^2}{d^3}. \tag{3}$$

In case of exponential distribution of traps, it can be assumed that the trapped hole carrier density (p_t) $\gg$ free charge carrier density (p_f) and using continuity equation and boundary condition, the current density (J) and applied voltage (V) can be expressed as[15]

$$J = q\mu p(x)E(x), \tag{4}$$

$$V = \int E(x)dx, \tag{5}$$

where $E(x)$ is the electric field inside the film. Further, the exponential distribution of traps in energy and space is given as

$$P(E) = N(E)E_t = H_t\exp\left(-\frac{E}{E_t}\right). \tag{6}$$

The expression for J is given by[15,18–23]

$$J = q^{1-l}\mu N_v\left(\frac{2l+1}{l+1}\right)^{l+1}\left(\frac{l}{l+1}\frac{\varepsilon_r\varepsilon_0}{N_t}\right)^l\frac{V^{l+1}}{d^{2l+1}}, \tag{7}$$

where $P(E)$ is the distribution function of hole trap density at an energy level E above the valence band (VB) edge, H_t is the trap density per unit energy range at the valence VB edge, N_t is the total trap density at the edge of VB and N_v is the effective density of states in the VB. E_t is the characteristic energy of the trap distribution, which determines the width of exponential trap state distribution that is often expressed in terms of the characteristic temperature T_c as $E_t = k_BT_c$ and $l = E_t/k_BT = T_c/T$, where k_B is the Boltzmann constant.[15,18] At $E = E_t$, we get from Eq. (6), $P(E_t)/H_t = 1/e$, which states that the trap energy level that characterizes the exponential distribution is defined as the energy at which the density of traps has been reduced by 1/e, as compared to the trap density at the VB edge.[18,24]

After performing some simple algebraic calculation, we rewrite Eq. (7) in its Arrhenius form to bring out the dependence of current density on temperature. Apply the exponential function to a natural logarithm without altering the results. Grouping together all the terms with $l = T_c/T$ from Eq. (7), we obtain[18,25]

$$J = \frac{q\mu_pN_vV}{L}\exp\left\{-\frac{E_t}{k_BT}\ln\left[\left(\frac{2l+1}{l+1}\right)^{-1/l}\frac{(l+1)^2}{l(2l+1)}\frac{qL^2N_t}{\varepsilon\varepsilon_0V}\right]\right\}. \tag{8}$$

For an exponential distribution of traps, the quasi-Fermi level, which depends on the magnitude of stored charge and hence on the applied voltage, is given by[18,25]

$$E_F(V) = k_BT_l\ln\left[f(l)\frac{qL^2N_t}{\varepsilon\varepsilon_0} - \ln V\right], \tag{9}$$

$$f(l) = \left(\frac{2l+1}{l+1}\right)^{-1/l}\frac{(l+1)^2}{l(2l+1)}, \tag{10}$$

where L is the thickness of the film, $f(l)$ is the pre-factor with l in Eq. (10), and is constant for any given temperature, where the power law $J \sim V^m$, $m > 2$ is satisfied. In the SCLC regime, E_F is thus linearly dependent on $\ln V$. The quasi-Fermi level $E_F(V)$ will coincide with the VB edge ($E_F = 0$), only if the right-hand side of Eq. (9) is zero.[18,25]

$$V = V_c = f(l)\frac{qL^2N_t}{\varepsilon\varepsilon_0}. \quad (11)$$

At the applied bias voltage $V = V_c$, all the traps are filled and E_F coincides with the VB edge energy E_{vb}. In organic semiconductor (polymer system), the conduction band (CB) and VB are represented by the LUMO and HOMO levels, respectively.

Temperature dependent steady state *J-V* characteristics for PTB7, PCDTBT and PTB7:PCDTBT blend in the configuration of ITO/PEDOT:PSS/polymer film/Au are shown in Figures 2(a), 2(b), and 2(c). At low applied voltages, the *J-V* characteristics exhibit ohmic behavior given by Eq. (1) in all the cases, as the injected carrier density is negligible as compared to background thermally generated carriers. In intermediate and higher voltage range, it is observed that the *J-V* characteristics follow the trap free SCLC (TF-SCLC) mechanism given by Eq. (3) near room temperature (280 K) in all the cases. It is expected, because the E_t (given in the Table I) is nearly equal to thermal activation energy, and the free carrier density is greater than trapped carriers density. Thus, all the traps are practically detrapped and play no role in the conduction of charge carriers.[14] The calculated hole mobility of PTB7, PCDTBT and PTB7:PCDTBT blend is $3.9 \times 10^{-4}\,cm^2\,V^{-1}\,s^{-1}$, $2.2 \times 10^{-4}\,cm^2\,V^{-1}\,s^{-1}$ and $9.19 \times 10^{-4}\,cm^2\,V^{-1}\,s^{-1}$, respectively, for $d = 240$ nm, $\varepsilon_r = 3$ and $\varepsilon_0 = 8.85 \times 10^{-14}$ F/cm.

In 240–160 K temperature range (Figure 2(a)), the slope of the *J-V* curve is 2 in intermediate and higher voltage range. It shows the presence of shallow traps located at a discrete energy level above the VB edge.[24] In such a case, the free carrier concentration is sufficient to fill all the traps, and the curve follows the TF-SCLC mechanism (Eq. (3)). The calculated hole mobilities at 240 K, 200 K and 160 K temperatures are 2.0×10^{-4}, 1.5×10^{-4} and $1.1 \times 10^{-4}\,cm^2\,V^{-1}\,s^{-1}$, respectively. At 140 K and 120 K, the *J-V* characteristic (inset Figure 2(a)) slope is greater than 2, and it follows the trap limited SCLC (TL-SCLC) and fits quite well with Eq. (7). Solid curves in the inset of Figure 2(a) represent the plot of Eq. (7) at their respective temperatures with $\mu = 9.0 \times 10^{-5}$ and $8.1 \times 10^{-5}\,cm^2\,V^{-1}\,s^{-1}$, respectively.

In 240–120 K temperature range (Figure 2(b)), the slope of *J-V* curve is >2, indicating the presence of deep traps,[24] and thermal energy is not sufficient to fill those traps. The *J-V* characteristics follow the TL-SCLC and are in good agreement with Eq. (7). The *J-V* characteristics at 240 K, 200 K, 160 K, 140 K and 120 K were fitted with $\mu = 1.25 \times 10^{-4}$, 1.2×10^{-4}, 1.15×10^{-4}, 1.1×10^{-4} and $9.6 \times 10^{-5}\,cm^2\,V^{-1}\,s^{-1}$, respectively.

In 240–160 K temperature range (Figure 2(c)), the slope of *J-V* curve is 2, and it shows the TF-SCLC behavior (Eq. (3)) at higher voltage. In this case, the concentration of free carrier becomes greater than trapped carriers. But, in the intermediate voltage range, the *J-V* curve (slope > 2) shows TL-SCLC (Eq. (7)). The characteristics measured at 240 K, 200 K, 160 K and 140 K were fitted with hole mobility $\mu = 8.01 \times 10^{-4}$, 7.8×10^{-4}, 7.38×10^{-4} and $6.44 \times 10^{-4}\,cm^2\,V^{-1}\,s^{-1}$, respectively. The other calculated parameters for PTB7, PCDTBT and PTB7:PCDTBT blend are shown in Table II. In the case of PTB7:PCDTBT (0.7:0.3) blend thin film, the mobility has been observed to be significantly higher than that of pristine PCDTBT and PTB7 at all measured temperatures (Figure 2(d)). It is seen from Table II that the charge transport parameters get significantly modulated in PTB7:PCDTBT blended film. The increase in μ can be attributed to the suppression in overall N_t, which results in a reduction in the V_c and strong modulation of the polymer-polymer energy levels (as seen by modulation of V_{oc}).[26]

TABLE II. Values of the transport parameters for the devices under study.

Polymer film	V_c (V)	N_t (cm^{-3})	E_t (meV)	μ at 280 K ($cm^2\,V^{-1}\,s^{-1}$)
PTB7	19	1.1×10^{17}	19.81	3.9×10^{-4}
PCDTBT	28	1.6×10^{17}	25.93	2.1×10^{-4}
PTB7:PCDTBT	13	7.4×10^{16}	23.69	9.1×10^{-4}

Morphology of the active layer plays a significant role in determining the transport properties of the polymers. In order to understand the role of morphology in decreasing the trap density of the polymer films, atomic force microscopy (AFM) is carried out. Figures 3(a), 3(b), and 3(c) show the morphology of the active layers of PTB7, PCDTBT and PTB7:PCDTBT (0.7:0.3) blend, respectively. From Figure 3(a), it is clearly observed that the morphology of pristine PTB7 film is not uniform due to the aggregation, and the root mean square (rms) value is 1.1 nm. This aggregation acts as trap state and plays an important role in the transport of charge carriers. Similarly, the pure PCDTBT also shows aggregation with the rms of 0.9 nm (Figure 3(b)). In the blend of PTB7:PCDTBT (Figure 3(c)), there is a marked decrease in the roughness to 0.5 nm, and there is almost no aggregation. It implies that blending of PCDTBT in PTB7 reduces aggregation and roughness, which improves the morphology and reduces the trap states that can have significant influence on the mobility and charge recombination. Therefore, the dependence of V_{oc} and J_{sc} in PTB7:PC_{71}BM (1:1.5), PCDTBT:PC_{71}BM (1:4) and PTB7:PCDTBT:PC_{71}BM (0.7:0.3:2) BHJ solar cells at various incident light (I_{light}) intensities were studied.

J_{sc} can be correlated to I_{light} as $J_{sc} \propto (I_{ligtht})^{\alpha}$ ($\alpha \leq 1$), where α is the exponential factor. Linear dependence of J_{sc} on light intensity with α value close to 1 shows the weak bimolecular recombination in the device.[27–29] At short circuit, the bimolecular recombination should be minimum ($\alpha \approx 1$) for maximum carrier sweep out. Figure 4(a) shows the J_{sc} *vs.* I_{light} plot on log-log scale fitted using the power law described above. The fitting of the data yields α values of 0.964, 0.914 and 0.995 for PTB7:PC_{71}BM (1:1.5), PCDTBT:PC_{71}BM (1:4) and PTB7:PCDTBT:PC_{71}BM (0.7:0.3:2), respectively. The

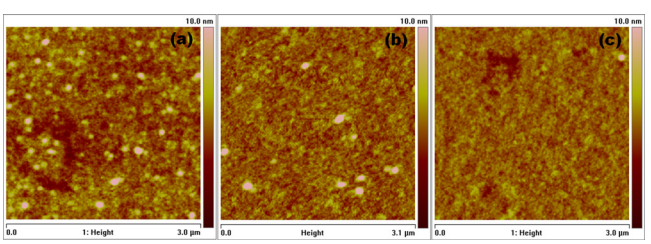

FIG. 3. Tapping mode AFM images of polymer films: (a) PTB7, (b) PCDTBT and (c) PTB7:PCDTBT (0.7:0.3) blend.

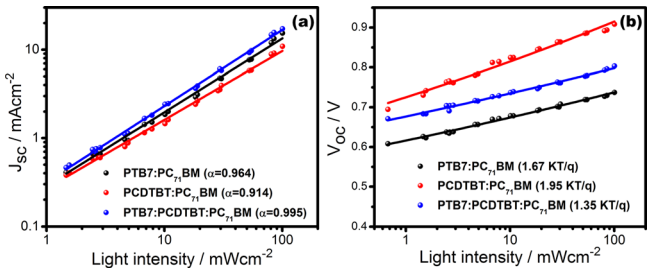

FIG. 4. Recombination study of the binary (PTB7:$PC_{71}BM$, PCDTBT:$PC_{71}BM$) and ternary device (PTB7:PCDTBT: $PC_{71}BM$). (a) Measured J_{sc} as a function of light intensity (symbol) on logarithmic scale and fitted power law (line yield α). (b) The measured V_{oc} as a function of light intensity (symbols) and together fitted with liner fits to data (solid lines).

slightly larger α value of PTB7:PCDTBT:$PC_{71}BM$ (0.7:0.3:2) devices indicates that the blending of PCDTBT with PTB7:$PC_{71}BM$ system leads to a decrease in bimolecular recombination. This is consistent with the increased shunt resistance in the PTB7:PCDTBT:$PC_{71}BM$ (0.7:0.3:2) solar cell (Table I).

Figure 4(b) demonstrates the dependence of V_{oc} on light intensity. The slope of V_{oc} versus ln(I_{light}) defines the degree of trap-assisted or Shockley–Read–Hall (SRH) recombination in the polymer solar cell. A slope at k_BT/q indicates the dominance of bimolecular recombination, where k_B is Boltzmann's constant, T is the temperature and q is the elementary charge. In trap-assisted recombination, it is observed that V_{oc} strongly depends upon light intensity with the slope $2kT/q$.[27–29] In the present case, PTB7:$PC_{71}BM$ and PCDTBT:$PC_{71}BM$ devices showed a slope of $1.67kT/q$ and $1.95kT/q$, respectively, while PTB7:PCDTBT:$PC_{71}BM$ device attained smaller slope $1.35kT/q$ as shown in Figure 4(b). Therefore, the blending of the PCDTBT in PTB7 significantly reduces the trap assisted recombination with a reduced slope of $1.35kT/q$. This is consistent with the decreased series resistance (Table I), which is a direct evidence of the reduced recombination and improved device performance.

In conclusion, charge transport properties reveal that there is a significant increase in hole mobility in the PTB7:PCDTBT blend. The increase in mobility is due to the improvement in morphology and suppressed trap states, and therefore, the charge extraction is better and recombination is reduced. This results in an increased J_{sc} and fill factor, whereas V_{oc} in the blend of PTB7:PCDTBT:$PC_{71}BM$ device is modulated as compared to the V_{oc} of the individual polymers, and therefore, the performance of ternary blend BHJ polymer solar cells is significantly improved.

The authors are grateful to the director, CSIR-National Physical Laboratory, New Delhi, India, for his encouragement. V.B. is grateful to University Grant Commission, Government of India for SRF fellowship. A.S. fellowship is supported by CSIR-TAPSUN (NWP-54) program. All authors are thankful to the CSIR-TAPSUN (NWP-54) program. Author acknowledges the technical support of Sandeep Singh, Ramil Bharadwaj and Neeraj Chaudhary.

[1]Y. Liu, J. Zhao, Z. Li, C. Mu, W. Ma, H. Hu, K. Jiang, H. Lin, H. Ade, and H. Yan, Nat. Commun. **5**, 5293 (2014).
[2]Z. He, B. Xiao, F. Liu, H. Wu, Y. Yang, S. Xiao, C. Wang, T. P. Russell, and Y. Cao, Nat. Photonics **9**, 174 (2015).
[3]Q. An, F. Zhang, J. Zhang, W. Tang, Z. Deng, and B. Hu, Energy Environ. Sci. **9**, 281 (2016).
[4]T. Ameri, P. Khoram, J. Min, and C. J. Brabec, Adv. Mater. **25**, 4245 (2013).
[5]L. Lu, T. Xu, W. Chen, E. S. Landry, and L. Yu, Nat. Photonics **8**, 716 (2014).
[6]V. Gupta, V. Bharti, M. Kumar, S. Chand, and A. J. Heeger, Adv. Mater. **27**, 4398 (2015).
[7]L. Lu, W. Chen, T. Xu, and L. Yu, Nat. Commun. **6**, 7327 (2015).
[8]P. P. Khlyabich, B. Burkhart, and B. C. Thompson, J. Am. Chem. Soc. **133**, 14534 (2011).
[9]P. Cheng, Y. Li, and X. Zhan, Energy Environ. Sci. **7**, 2005 (2014).
[10]T. Goh, J.-Sh. Huang, B. Bartolome, M. Y. Sfeir, M. Vaisman, M. L. Lee, and A. D. Taylor, J. Mater. Chem. A **3**, 18611 (2015).
[11]W.-L. Xu, B. Wu, F. Zheng, X.-Yu. Yang, H.-D. Jin, F. Zhu, and X.-T. Hao, J. Phys. Chem. C **119**, 21913 (2015).
[12]Y. Yang, W. Chen, L. Dou, W.-H. Chang, H.-S. Duan, B. Bob, G. Li, and Y. Yang, Nat. Photonics **9**, 190 (2015).
[13]S. C. Jain, A. K. Kapoor, W. Geens, J. Poortmans, R. Mertens, and M. Willander, J. Appl. Phys. **92**, 3752 (2002).
[14]P. Kumar, S. Chand, S. Dwivedi, and M. N. Kamalasanan, Appl. Phys. Lett. **90**, 023501 (2007).
[15]K.-C. Kao and W. Hwang, *Electrical Transport in Solids: With Particular Reference to Organic Semiconductors* (Taylor & Francis, 1979), p. 160.
[16]P. W. M. Blom, M. J. M. de Jong, and M. G. van Munster, Phys. Rev. B **55**, R656 (1997).
[17]T. van Woudenbergh, P. W. M. Blom, M. C. J. M. Vissenberg, and J. N. Huiberts, Appl. Phys. Lett. **79**, 1697 (2001).
[18]Z. Chiguvare and V. Dyakonov, Phys. Rev. B **70**, 235207 (2004).
[19]K. Kumari, S. Chand, P. Kumar, S. N. Sharma, V. D. Vankar, and V. Kumar, Appl. Phys. Lett. **92**, 263504 (2008).
[20]M. Planells, A. Abate, D. J. Hollman, S. D. Stranks, V. Bharti, J. Gaur, D. Mohanty, S. Chand, H. J. Snaith, and N. Robertson, J. Mater. Chem. A **1**, 6949 (2013).
[21]A. Abate, M. Planells, D. J. Hollman, V. Bharti, S. Chand, H. J. Snaith, and N. Robertson, Phys. Chem. Chem. Phys. **17**(4), 2335 (2015).
[22]N. F. Mott and R. W. Gurney, *Electronic Processes in Ionic Crystals* (Oxford, London, 1940).
[23]M. A. Lampert and P. Mark, *Current Injection in Solids* (Academic, New York, 1970), p. 76.
[24]S. Biswas, B. Dutta, and S. Bhattacharya, J. Appl. Phys. **114**, 143701 (2013).
[25]V. Kumar, S. C. Jain, A. K. Kapoor, J. Poortmans, and R. Mertens, J. Appl. Phys. **94**, 1283 (2003).
[26]N. Felekidis, E. Wang, and M. Kemerink, Energy Environ. Sci. **9**, 257 (2016).
[27]L. J. A. Koster, V. D. Mihailetchi, R. Ramaker, and P. W. M. Blom, Appl. Phys. Lett. **86**, 123509 (2005).
[28]S. R. Cowan, A. Roy, and A. J. Heeger, Phys. Rev. B **82**, 245207 (2010).
[29]V. Gupta, A. K. K. Kyaw, D. H. Wang, S. Chand, G. C. Bazan, and A. J. Heeger, Sci. Rep. **3**, 1965 (2013).